Poly(-caprolactone)/bioactive glass composite electrospun fibers for tissue engineering applications

Received: 21 December 2022 | Revised: 23 May 2023 | Accepted: 27 May 2023

DOI: 10.1002/jbm.a.37578

RESEARCH ARTICLE

Society For Biomaterials | WILEY

Poly(ε-caprolactone)/bioactive glass composite electrospun fibers for tissue engineering applications

Elisa Piatti[1] | Marta Miola[1] | Liliana Liverani[2,3] | Enrica Verné[1] | Aldo R. Boccaccini[2]

[1]Department of Applied Science and Technology (DISAT), Politecnico di Torino, Turin, Italy

[2]Department of Materials Science and Engineering, Institute of Biomaterials, University of Erlangen-Nürnberg, Erlangen, Germany

[3]DGS S.p.A., Rome, Italy

Correspondence
Marta Miola, Department of Applied Science and Technology (DISAT), Politecnico di Torino, Corso Duca degli Abruzzi 24, 10129 Turin, Italy.
Email: marta.miola@polito.it

Abstract

In this work, composite electrospun fibers containing innovative bioactive glass nanoparticles were produced and characterized. Poly(ε-caprolactone), benign solvents, and sol–gel B- and Cu-doped bioactive glass powders were used to fabricate fibrous scaffolds. The retention of bioactive glass nanoparticles in the polymer matrix, the electrospinnability of this novel solution and the obtained electrospun composites were extensively characterized. As a result, composite electrospun fibers characterized by biocompatibility, bioactivity, and exhibiting overall properties adequate for both hard and soft tissue engineering applications, have been produced. The addition of these bioactive glass nanoparticles was, indeed, able to impart bioactive properties to the fibers. Cell culture studies show promising results, demonstrating proliferation and growth of cells on the composite fibers. Wettability, degradation rate, and mechanical performance were also tested and are in line with previous results.

KEYWORDS

benign solvents, bioactive glass, boron, composite, copper, electrospinning, poly(epsilon-caprolactone)

1 | INTRODUCTION

Tissue engineering (TE) and regenerative medicine represent promising therapeutic alternative approaches to the transplant of organs and tissues with the aim of repairing and regenerating diseased or damaged living human tissues, overcoming the problems of deficiency of donor tissue and potential donor site morbidity.[1,2] In this context, the use of an engineered scaffold as a temporary template for supporting tissue regeneration is of fundamental importance.[3–5] Indeed, scaffolds play a key role in TE, allowing cells to adhere, proliferate, differentiate and form new normal and healthy tissues during the gradual degradation of the scaffolds.[4] In order to face a complex biological system as the human body, a scaffold must fulfill several extremely challenging requirements that depend on the final application,[4,6,7] such as biocompatibility, bioactivity, open porous structure with a controllable inter-connected porosity and the ability to promote attachment, differentiation, and proliferation of human cells. Moreover, the in vivo biodegradation rate of the scaffold should be tailored in order to match the regeneration rate of the damaged tissue and guarantee the formation of non-toxic degradation products that can be easily expelled by the body, for example via the lymphatic, respiratory, or urine systems. This tailoring can be achieved by an appropriate design of the composition, structure, and porosity of the scaffold. The scaffold should also assure structural and mechanical matching with the host tissue, avoiding that the scaffold could collapse during scaffold handling and providing physical support to the tissue under regeneration until the mechanical integrity of the new tissue is sufficient to guarantee its own support. Finally, the scaffold fabrication process should assure easy near-net-shape and scalability.[1]

Degradable biomaterials are optimal options for developing TE scaffolds which must progressively degrade during new tissue formation.[4]

Synthetic bioactive and bioresorbable composite materials have attracted considerable interest as materials for the fabrication of scaffolds for TE.[8] Among others, composite materials formed by the combination of bioactive inorganic phases (such as hydroxyapatite [HA], calcium phosphates [CaP], bioactive glasses [BGs] and biodegradable polymers are gaining increasing attention).[1,8] In particular, synthetic biodegradable polymers are among the most largely investigated materials for the development of TE scaffolds.[8] Among this class of polymers, aliphatic polyesters, such as poly-ε(caprolactone) (PCL), polyethylene oxide (PEO), poly(3-hydroxybutytrate) (PHB), polylactic acid (PLA), polyglycolic acid (PGA), their copolymers and blends, are approved by the USA Food and Drug Administration (FDA).[2,8–10] Their advantages are the predictability and reproducibility of the mechanical and physical properties, the low risks of toxicity, immunogenicity and infections, and the chemical hydrolytic degradation, which occurs by hydrolysis of ester bonds (de-esterification) after water uptake, without any variations from patient to patient.[4,8,9] Moreover, using these polymers, scaffolds with complex shapes and structures can be easily fabricated, but unfortunately, generally, they are not able to exert a bioactive behavior (e.g., strong bonding to living tissues and good cell adhesion, as a consequence of their hydrophobic nature) and are too flexible and weak to satisfy the mechanical requirements that are necessary for surgery and in the human body.[8,11] Furthermore, during their hydrolytic degradation process, biodegradable polymers release acid products, that lower the pH of the environment close to the polymer, hence leading to an acceleration of the degradation in an autocatalytic manner, that can arise adverse tissue reactions, such as inflammation and in vivo foreign body reactions.[8,9] The incorporation in the polymer matrix of compounds that can affect the pH toward alkaline values (such as BGs) can exploit a buffering effect on the acidity of the polymer degradation products and regulate their degradation rate,[4,8] by rapidly exchanging protons in water with alkaline ions in their network.[8,12] In this way, due to the pH buffering effect, the formation of a favorable environment for cells can be achieved (on the contrary, low pH values are unfavorable for cells).[4] The fabrication of composites with a polymeric matrix embedding BGs is thus desirable because they can take at the same time advantages of the good properties of both materials and minimize their shortcomings.[1,4,8,13,14] In particular, nanosized BG particles are considered as ideal fillers for TE scaffolds.[4,15]

BGs are non-crystalline solids able to bond with both hard and soft tissues. Since their discovery, they were used for bone regeneration, but more recently they are gaining increasing attention for the possibility to use them for soft tissue regeneration (such as regeneration of skin, tendons, muscles, articular cartilage, nerves, intervertebral disc, joint capsule, and blood vessels), as shown by many experimental studies.[1,16,17]

The combination of polymers and BGs can be achieved by preparing composite materials using different fabrication methods, as largely reviewed.[4,8] In particular, to produce fibrous scaffolds which mimic the fibrous structure of the extracellular matrix (ECM),[18] the electrospinning technique is widely used.[19,20] The electrospinning method offers several advantages for the fabrication of polymeric fibers.[9,21–24] This technique is, in fact, simple, cost-effective, versatile, tunable, and scalable, allowing to fabricate scaffolds using a huge number of viscoelastic polymers and their blends and to incorporate easily several inorganic phases and functional components (like drugs, genes, enzymes, and living cells).[19,20] In addition, the properties of the electrospun fibers can be easily adjusted in accordance with the purpose of their use. Thus, using the electrospinning technique, it is possible to synthetize thin non-woven continuous fibers with fibrillar structure and diameters in the range of sub-micrometers down to nanometers, characterized by a high aspect ratio, high surface area, and high interconnected porosity, which can be organized in the form of 3D macroporous materials for potential TE applications. Anyway, despite its numerous advantageous properties, the electrospinning process is limited by the use of toxic solvents that may cause adverse effects to cells if not removed completely, difficulty in controlling pore size and pore shape, safety problems for the lab workers and negative environmental impact.[21] For this reason, recently, the idea of "green electrospinning" involving the use of less or not toxic solvents (benign solvents for electrospinning, according to the definition reported in Reference 25) is currently applied in several works.[21,26–28]

In a similar scenario, the incorporation of bioactive glasses and/or drugs promoting the formation of new blood vessels (angiogenesis) is of extreme interest.[29,30] Indeed, to allow gas exchange, delivery of soluble signaling molecules (like growth factors GFs) and nutrients, and removal of waste products, an adequate capillary network is necessary for both hard and soft tissue regeneration, especially if regenerating tissues in volumes greater than a few mm^3.[9] Besides lacking vascularization, infections are a serious problem for the success of each implant. Moreover, it is possible to accelerate the repair and the regeneration of damaged tissues, only by (a) increasing cell proliferation, (b) reducing inflammation, (c) improving angiogenesis, and (d) imparting antibacterial properties to the scaffold.[30] Up to now, BGs with many different compositions containing doping elements such as boron,[28] cerium,[31] cobalt,[32] gallium,[31] and silver[28,32,33] have already been incorporated in PCL fibrous scaffolds in order to impart angiogenic and antibacterial properties to the neat polymeric scaffolds for their use for TE applications, such as wound healing.

In this context, the aim of the present work was the synthesis of electrospun composite fibers containing BG nanoparticles co-doped with boron and copper, in order to impart both pro-angiogenic and antibacterial properties to the composites. It has been largely demonstrated that boron possesses pro-angiogenetic properties and can stimulate the formation of new blood vessels and the regeneration of soft tissues, such as skin.[30,34,35] On the other hand, copper is one of the most studied antibacterial ions, able to obstacle bacterial infections.[36–38] In a previous work[39] innovative silica-based bioactive glasses co-doped with boron and copper by an unconventional sol–gel route have been designed and characterized, showing promising potential applications in the TE field. The novelty of the present work lies in the incorporation of the innovative sol–gel BGs designed in Reference 39 in polymeric electrospun fibers and on the evaluation of the interaction of these new glass nanoparticles with the polymeric system to understand the suitability of this composite material for hard and soft TE applications.

2 | MATERIALS AND METHODS

2.1 | Materials

For the electrospinning solution, poly(ε-caprolactone) (PCL, 80 kDa, Sigma Aldrich, Munich, Germany) was used for the biopolymer matrix and acetic acid at 98% (AA, VWR, Germany) was used as the solvent. In order to synthesize composite fibrous materials, three different bioactive glasses with nominal compositions of 77%SiO_2–9%P_2O_5–14%CaO (wt%, S2 glass), 62%SiO_2–9%P_2O_5–14%CaO–15%B_2O_3 (wt%, SB2 glass) and 62%SiO_2–9%P_2O_5–9%CaO–5%CuO–15%B_2O_3 (wt%, SBCu2 glass) were properly designed and synthetized, as previously reported.[39]

2.2 | Synthesis of the BG powders

The preparation of the BG nanoparticles was achieved by following a previously described procedure.[39] Briefly, the silica precursor (tetraethyl orthosilicate, TEOS) was hydrolyzed in a mixture of ethanol, water, and nitric acid (HNO_3 2 M), magnetically stirring at room temperature for 1 h. In detail, a solution of 30 mL of EtOH, 7.2 mL of H_2O, 1.2 mL of HNO_3 2 M and 11.2 mL of TEOS was prepared and left under gentle and constant magnetic stirring for 1 h. Then, all other precursors (triethyl phosphate, TEP, for phosphorus, calcium nitrate tetrahydrate $Ca(NO_3)_2{\cdot}4\ H_2O$ for calcium, copper nitrate trihydrate $Cu(NO_3)_2{\cdot}3\ H_2O$ and boric acid H_3BO_3 for boron) were added separately with a time interval of 30 min between each precursor addition, while continuously magnetically stirring, following a fixed order: 1.04 mL of TEP, 1.85 g of $Ca(NO_3)_2{\cdot}4\ H_2O$, 0.74 g of $Cu(NO_3)_2{\cdot}3\ H_2O$ and 1.30 g of H_3BO_3. Half an hour after the addition of the last precursor, NH_4OH 2 M was added dropwise under vigorous stirring until the pH reached a value in the range of 8–9, leading to the formation of a gel, which was later dried at 60°C for 48 h in a heater and calcinated at 700°C for 2 h in a furnace.

2.3 | Synthesis of the composites

The above-mentioned new sol–gel BG particles were incorporated in PCL fibers for the first time in this work. Thus, because of the novelty of the incorporation of such new sol–gel BG particles in a PCL matrix, it was necessary to optimize the glass addition protocol in order to successfully disperse these BG particles in the PCL solution. Thus, various solvent systems and different mixing methods were tried to add the BG particles and obtain the most homogenous electrospinning solution as possible. The first attempt was done with a solution (15 wt/v%) of PCL in a mixture of formic acid (FA) and acetic acid (AA), which was previously successfully used to electrospun PCL nanofibers, using a voltage of 20 kV, a working distance of 11 cm and a flow rate of 0.67 mL/h.[21] In detail, PCL was dissolved at 15 wt/v% in a mixture of acetic acid (AA) and formic acid (FA) during continuous stirring, until a transparent solution was obtained. However, due to the residual glass aggregates, a second approach with only AA, already used in previous experimental works,[25,40] was preferred. Thus, PCL was dissolved in AA (at 20 w/v%), mixing overnight at 30°C until the solution became clear, and then ultrasonicated for 1 h to obtain a homogeneous solution.[21] As expected, the agglomerated nanoparticles seemed to be better linked to the PCL fibers.

Taking into account the critical threshold range of BG content (5–40 wt%), which is necessary for optimal osteoblast growth and Ca–P formation in a composite scaffold,[1] different glass concentrations (5%, 10%, 20%, and 30%) were used to investigate the electrospinnability of the glass/polymer dispersion, the effect of glass incorporation inside the PCL matrix and the bioactivity of the composite fibers. Finally, a BG content of 20% (wt/wt%) was selected. Thus, for the synthesis of composite fibrous materials, 20% of glass powders (wt/wt%, in relation to the PCL amount) was added and mixed with the PCL solution, following an optimized protocol. In detail, 2 min of manual mixing, 5 min of magnetic stirring and 1 min in an ultrasonic (US) bath, in order to disperse the glass particles and destroy agglomerates. This mixing method was selected for its reproducibility, speed and ability to produce an electrospinning solution with a satisfactory particle dispersion, after having tried many other methods, such as (a) 10 min of magnetic stirring and 1 min in US bath, (b) manual mixing for 2 and 1 min in US bath, (c) addition of glass powders in 1 mL of the mixture of acetic acid and formic acid, followed by manual mixing and later addition in the polymer solution (glass dispersion method), and (d) method similar to the previous one, but mixing the glass powders with Pluronic (1% wt/wt) in the mixture of AA and FA.[40]

Electrospinning was performed by using a horizontal commercially available electrospinning setup (Starter Kit 40 KV Web, Linari srl, Italy), BD plastic syringes of 3 mL with a cross-section of 0.589 cm^2 and needles of 21 G × 7/8″. All electrospinning experiments were carried out at room temperature in air. Environmental parameters, such as temperature (T) and relative humidity (RH) were checked, but it was not possible to control them, because the device was not equipped with climate control to allow the setting and control of T and RH inside the electrospinning chamber.

Neat PCL fibers were synthesized as control, in agreement with previous experimental works of Liverani and Boccaccini.[21]

It is well known in literature[32,41] that the addition of BG powders or particles in a polymeric solution can alter the electrospinnability of the solution, by modifying the viscosity and the conductibility of the electrospinning solution, among others. So, a time-consuming optimization process, was necessary in order to select the best process parameters for the synthesis of the composite fibers. Finally, the following electrospinning parameters were selected for the electrospinning suspension containing the BGs: 11 cm as working distance, 15 kV as applied voltage, 0.4 mL/h (when S2 and SB2 glass particles were used) and 0.7 mL/h (when SBCu2 glass particles were used) as flow rate.

The fabricated materials are reported in Table 1.

TABLE 1 List of electrospun fibers and parameters used for electrospinning.

Sample name	Polymer	Solvent	Glass used as filler (if used)	Amount of glass (wt% with respect to polymer)	Applied voltage (kV)	Working distance (cm)	Flow rate (mL/h)
PCL/AA	PCL	Acetic acid	No filler (neat PCL fibers)	0%	15	11	0.4
PCL/AA/S2	PCL	Acetic acid	S2	20%	15	11	0.4
PCL/AA/SB2	PCL	Acetic acid	SB2	20%	15	11	0.4
PCL/AA/SBCu2	PCL	Acetic acid	SBCu2	20%	15	11	0.7

2.4 | Morphological and compositional characterization

To assess the morphological and compositional properties of the electrospun fibers, scanning electron microscopy was performed using a field-emission scanning electron microscope (FESEM Auriga, Carl-Zeiss, Germany), equipped with energy dispersive spectroscopy (EDS) device. To perform the analysis, a small section of the fibers was carefully sectioned and fixed onto a SEM holder using a double carbon tape, and then sputtered with chromium. Fiber average diameters were measured by using the software ImageJ analysis software (NIH, USA)[42] on SEM micrographs. EDS was used to evaluate glass incorporation and glass distribution inside the composite fibrous membranes.

2.5 | ATR-FTIR analysis

For the evaluation of the incorporation of the BG nanoparticles inside the polymeric matrix, neat and composite membranes were characterized by Attenuated Total Reflectance-Fourier Transform Infrared (ATR-FTIR) spectroscopy, using the spectrometer Shimadzu IRAffinity-1S (Shimadzu Corp, Japan) in ATR mode, with a selected number of spectral scans of 40, a resolution of 4 cm^{-1} and a wavenumber range between 4000 and 400 cm^{-1}.

2.6 | Stability test

The BG nanoparticles were immersed up to 1 h in AA in the same ratio used for the electrospinning solution and then, after removing the acid, the glass powders were dried under a fume hood for 48 h. The treated glass powders were then analyzed by using FESEM (Auriga, Carl-Zeiss, Germany), FTIR (Shimadzu IRAffinity-1S, Shimadzu Corp, Japan), and X-ray diffraction (XRD) analysis (X'Pert diffractometer, Philips, Netherlands), to evaluate the interaction between the used glasses (S2, SB2 and SBCu2) and the used solvent (AA), in particular in terms of clustering and degradation of the glass particles.

Moreover, in order to confirm the bioactivity of S2, SB2 and SBCu2 glasses even after immersion in AA, an in vitro bioactivity test was carried out on the AA-immersed glass particles, soaking the BG powders (three samples) in a simulated body fluid (SBF), which is a particular solution, usually adopted to estimate the bioactivity of the glasses, characterized by the same pH and ionic concentration of the inorganic part of the human plasma, allowing to mimic the chemical reactions that would occur between the BGs and the human fluids in case of implant.[43] The SBF solution was prepared following the Kokubo protocol[43] and the in vitro acellular bioactivity test was carried out up to 14 days. The pH of each sample was measured after 1, 3, 7, 10, 12 and 14 days. At each time point, samples were removed from SBF solution, washed with distilled water (which was removed by centrifuging for 10 min at 5000 rpm), dried in a heater at 37°C and analyzed with FESEM (Gemini SUPRATM 40, Zeiss, Germany), equipped with EDS device, and XRD (X'Pert diffractometer, Philips, Netherlands). The XRD analysis was performed using the Bragg Brentano camera geometry, the Cu-Ka incident radiation, a source voltage of 40 kV, a current of 30 mA, an incident wavelength λ of 1.5405 Å, a step size $\Delta(2\theta)$ of 0.02°, a counting time of 1 s per step and an analysis degree 2θ varying between 10° and 70°. To analyze the recorded XRD spectra, the X'Pert HighScore program (equipped with PCPDFWIN database) was then used.

2.7 | Water contact-angle measurements

Surface wettability of fibrous structures was evaluated because it is well known that it has a strong impact on the attachment and adhesion of cells, on the expression of proteins, and on the subsequent tissue growth.[44–47] Indeed, different cells interact differently with hydrophilic or hydrophobic surfaces, being attracted or repelled by the implant surface.[48] Moreover, the hydrophilic or hydrophobic nature of the material influences the mechanism and the rate of its in vivo degradation.[8] Therefore, water contact angle measurements were performed on both neat and composite samples with a contact angle measurement device (Krüss DSA30, Hamburg, Germany), dropping 3 µL of distilled water onto the fibrous materials. The contact angle (CA) is, in fact, the angle between a liquid–vapor interface of the liquid drop and the wet solid surface. If the CA is smaller than 90°, the surface is hydrophilic, whereas if the CA is bigger than 90°, the surface is hydrophobic.[8]

At least three measurements were performed for each type of electrospun fibrous material and, in each measurement, the CA value was automatically measured every second in a time frame of 10 s for each tested sample.

2.8 | Mechanical characterization

The mechanical properties of the electrospun fibrous materials were determined by performing uniaxial tensile tests, which were carried out with a uniaxial testing machine (5967 Dual Column Tabletop Testing System, Instron®, Darmstadt, Germany) using a load cell of 50 N and a cross-head speed of 10 mm/min. All materials were cut in 3×20 mm^2 stripes and then fixed in a paper frame, as previously reported.[21] The inner dimension of this paper frame was 10×10 mm^2 whereas the external one was 20×20 mm^2. The thickness of the electrospun membranes was calculated by measuring it in 10 parts of each mat with a digital micrometer having a precision of 1 μm and then averaging the measured values. For major accuracy, this value was compared with the thickness of each stripe, which was measured in three parts of each sample with the same digital micrometer. Tensile properties were then calculated from the stress–strain curves obtained by the tensile measurements and reported in terms of average value and standard deviation. The stress σ could be calculated by dividing the applied force F by the area A on which the force was applied. The sample area was calculated as $b \times t$ where b is the width of the sample corresponding to the inner width of the frame which was used to perform the mechanical test and t is the thickness of the sample (which was in the range 0.05–0.06 mm for all the composite materials).

For each type of electrospun fibers, five samples were tested and the obtained results were averaged.

2.9 | In vitro bioactivity test

The in vitro bioactivity of the fiber mats was evaluated by immersing samples in SBF. Before the immersion in SBF, the electrospun samples were fixed on round scaffold supports (Scaffdex, Sigma Aldrich, Munich, Germany) that have a diameter of 1 cm. The SBF was prepared and the ratio between the sample surface and the SBF volume was calculated according to Kokubo's protocol.[43] In detail, for the ratio evaluation, the following equation was used: $V_S = S_{tot}/10$, where, V_S denotes the volume of SBF expressed in mL and S_{tot} is the surface area in terms of square millimeters, calculated as $S_{tot} = 2S$ (where S is the inner area of the Scaffdex, which represents the minimal useful area, which was multiplicated for 2 in order to consider both sides of the electrospun mats).

Different soaking times were evaluated, leaving the samples immersed in SBF at 37°C in an orbital shaker (KS 4000i control, IKA® Werke GmbH & Co. KG, Germany) on an oscillating tray of 120 rpm for 1, 3, 5, 7, 14 and 21 days, without renewing the SBF solution. An empty SBF solution and neat PCL fibers were used as a control. Three samples were tested for each time point.

At the end of each soaking time, the samples were removed from SBF, rinsed three times with deionized water, dried under fume-hood and analyzed using SEM-EDS (Jeol JCH-6000 plus, Jeol SPA, Italy, equipped with EDS device) and FTIR (Thermo Scientific Nicolet iS50 FT-IR Spectrometer equipped with OMNIC software). In order to analyze the specimens by SEM, a small section of the fibers was carefully sectioned and fixed onto a SEM holder using a double carbon tape, and then sputtered with chromium. Variations in solution pH were also evaluated during all the in vitro acellular bioactivity test, measuring the pH of the three samples at each time point.

2.10 | In vitro biodegradation test

To assess the biodegradability, the fibers were soaked in phosphate buffered saline (PBS) solution, which was prepared by dissolving a specific commercial tablet in 100 mL of distilled water. Before the immersion in PBS, each sample was fixed on a Scaffdex.

The necessary PBS volume ratio (calculated according to Kokubo's protocol[43]) and the sample supports were the same used for the in vitro acellular bioactivity test. The samples were incubated in an orbital shaker (KS 4000i control, IKA® Werke GmbH & Co. KG, Germany) at 37°C and at 90 rpm for 1 and 7 days. The maximal duration of the experiment was fixed to 1 week for comparison with previous literature in vitro biodegradation test on composite fibers.[49,50] The experiment was carried out in triplicate and, at each time point, the pH was measured for each sample. A falcon tube containing only PBS solution was used as a reference for pH measurements.

At the end of each time point (1 or 7 days in PBS), the samples were carefully rinsed three times with deionized water, dried under a fume hood and then analyzed using SEM and ATR-FTIR.

2.11 | Cytocompatibility test

In order to preliminary assess cell viability and morphology on the electrospun materials, a protocol adapted from a previous work[25] was used.

Bone murine stromal ST-2 cells (Leibniz-Institut DSMZ—German Collection of Microorganisns and Cell Cultures GmbH, Germany) were cultured in RPMI 1640 medium (Thermo Fisher Scientific), supplemented with 10% fetal bovine serum (Lonza) and 1% penicillin/streptomycin (Lonza) and incubated at 37°C with 5% CO_2 and then seeded on the electrospun materials, that were previously cut, fixed on appropriate sample holders (Scaffdex), as described in Section 2.9, put in 24-multiwell and disinfected by exposure to UV light for 1 h. The seeding on the electrospun materials was performed with drop seeding, in which a drop of 100 μL of cell suspension with an inoculum ratio of 1.65×10^5 cells/mL was placed in the center of the materials. Fifteen minutes after the deposition of the drop, 1 mL of RPMI medium was added to each well. Neat PCL electrospun fibers were used as control. Among the different commercially available colorimetric cell proliferation assays, commonly used to assess the biomaterials biocompatibility, WST-8 (WST-8 assay, CCK-8, Sigma Aldrich, Germany) was selected. The assay is based on the use of the highly water-soluble WST-8 tetrazolium

salt ([2-(2-methoxy-4-nitrophenyl)-3-(4-nitrophenyl)-5-(2,4-disulfophenyl)-2Htetrazolium, monosodium salt] [Patent No. WO97/38985]) which produces a water soluble formazan dye (orange color) upon reduction due to the cellular dehydrogenases. Therefore, the amount of produced formazan is proportional to the amount of living cells, and it was evaluated by measuring the absorbance (optical density, OD) at 450 nm, with a plate Elisa reader (PHOmo Elisa reader, Autobio Diagnostics Co. Ltd., Zhengzhou, China). The WST-8 assay was performed, selecting as time points for the analysis the first day and 7th day after the cell seeding; the cell medium was removed to measure the cell viability at each time points and it was also replaced 3 days after the cell seeding.

Fluorescence microscopy was used to investigate the morphology of the cells adhering to the substrate, using a fluorescent microscope (Axio Scope A1, Zeiss) and rhodamine phalloidin (ThermoFisher Scientific) and 4′,6-diamidino-2-phenylindole (DAPI) (ThermoFisher Scientific) for the staining of actin filament (visible in red) and cell nuclei (stained in blue), respectively. The protocol for the staining involves the initial immersion of the samples in a fixation solution (1,4-piperazinediethanesulfonic acid buffer, ethylene glycol tetra-acetic acid, polyethylene glycol, paraformaldehyde, PBS and sodium hydroxide, purchased by Sigma) and a permeabilization buffer, followed by the addition of rhodamine phalloidin and DAPI in the concentration of 8 and 1 μL/mL to each well, respectively.

2.12 | Statistical analysis

All results of fiber diameters, EDS and CA analyses, mechanical and cytocompatibility tests were expressed as (mean ± standard deviation). CA and mechanical results were analyzed by Student's *t*-test: $p < .05$ was considered significant; for cytocompatibility results one-way analysis of variance (ANOVA) was used and a p value <.05 was considered statistically significant.

3 | RESULTS AND DISCUSSION

3.1 | Morphological and compositional characterization

Figure 1 reports the FESEM images of composite fibers; the micrographs show the presence of glass particles and some aggregates between the fibers or emerging from the fibers (highlighted by red circles). Observing these images, it is clear that the use of a concentration of 20% of bioactive glass (wt/wt%) allowed the synthesis of composite electrospun fibrous structures with high glass content, as desired, although the glass particles (in general smaller than 100 nm and with average size around 50 nm) tended to agglomerate forming micrometric aggregates (of size reaching even about 20 μm in the

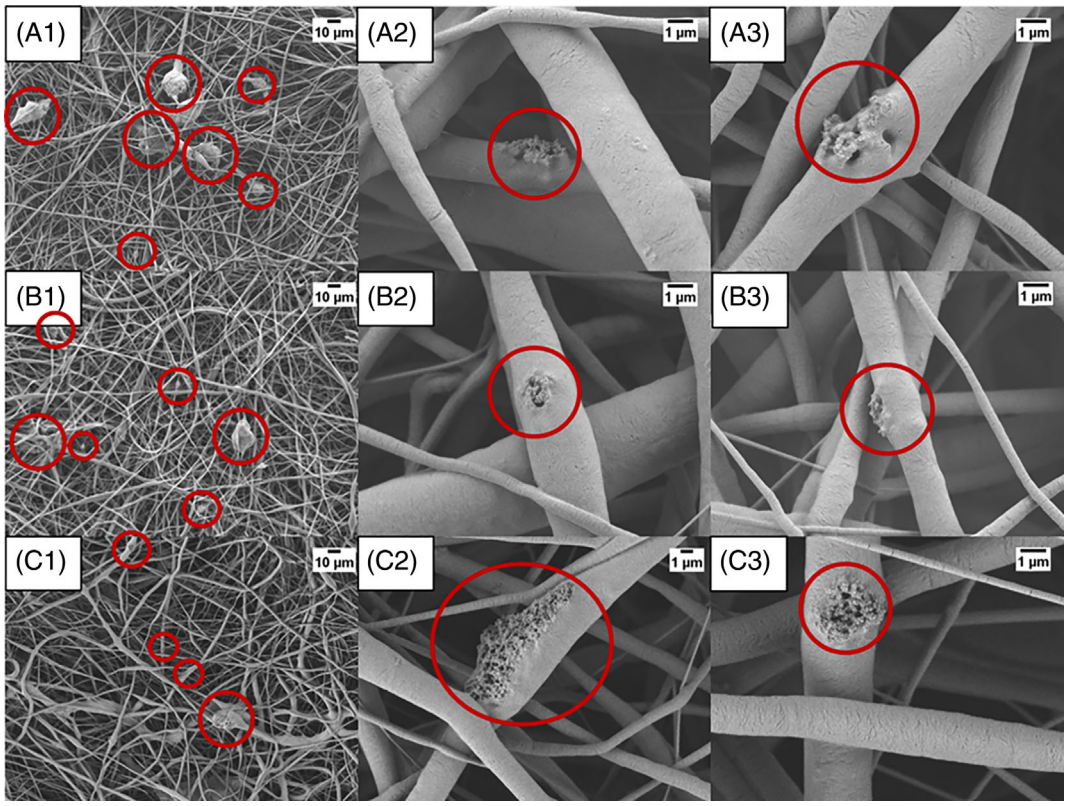

FIGURE 1 FESEM micrographs of PCL/AA/S2 (20%) fibers (A.1, A.2 and A.3), PCL/AA/SB2 (20%) fibers (B.1, B.2 and B.3) and PCL/AA/SBCu2 (20%) fibers (C.1, C.2 and C.3).

worst cases) and thus resulting in irregular distribution within the polymeric matrix, in agreement with previous results.[9]

In Table 2, the diameters of the synthetized composite fibers are reported in terms of average and standard deviation; the average was calculated as mean value of 30 measured fiber diameters, measured on two significant images. These values are comparable with data reported in literature, with the use of AA as benign solvent, resulting in beaded or microscale fibers.[51]

Although a significant increase in the diameter of the fibers was observed near the glass clusters (that sometimes come out from the fibers), no remarkable differences in fiber diameter values among the different types of composites were observed. Therefore, the composite fibers are characterized by the presence of some superficial agglomerated particles and smaller incorporated nanoparticles that caused a high surface roughness of the fibrous materials, in agreement with previous results of Moura et al.[32] suggesting that the BG particle distribution is not completely uniform.

Results of EDS area analysis (reported in the EDS maps and EDS spectrum in Figure 2) confirmed the incorporation of the BG nanoparticles in the PCL matrix, since the presence of silicon, calcium and phosphorus (the main elements of BGs) was noticed. The presence of boron was not detected because of limitations of EDS analysis itself. In any case, the presence of boron in these BGs was already proved in previous works.[39] Taking into consideration the similarities in glass granulometry and fiber morphology, EDS analysis was performed only in the case of PCL/AA/SB2 (20%) mat.

3.2 | ATR-FTIR analysis

The FTIR spectra of both the neat PCL and composite fibers (Figure 3) are characterized by the main PCL bands at 2943, 2866, 1722, 1294, 1240 and 1165 cm^{-1}, that can be attributed to asymmetric and symmetric CH_2 stretching, carbonyl (C═O) stretching, C—C stretching, asymmetric and symmetric C—O—C stretching, respectively[21,52] and that cover the bioactive glass peaks, hindering their identification, in agreement with results reported in literature.[32]

3.3 | Stability test

After immersion in AA, BG powders were observed with FESEM (not reported), showing that the glass nanoparticles maintained their morphology and a certain degree of agglomeration. However, a release of copper ions for SBCu2/AA samples probably occurred during immersion in AA. This Cu release could be the reason for the change in coloration of the glass particles, as exhibited in Figure 4A, and the differences in the XRD patterns before[39] and after the immersion in AA. In the XRD pattern of SBCu2 immersed in AA (SBCu2/AA), peaks related to copper acetate were identified, as shown in the upper graph in Figure 4B. The precipitation of this copper acetate on the BG nanoparticles after the immersion in AA can be considered as a proof of the release of Cu ions during the immersion in AA. These peaks disappeared after washing with bi-distilled water (as shown in the lower graph of Figure 4B).

Moreover, stability test results confirm that the used glasses were bioactive even after immersion in AA up to 1 h. Indeed, FESEM images (Figure 5) recorded on samples immersed in SBF for up to 14 days, compared with unsoaked SBCu2/AA, and pristine SBCu2 glasses, showed the formation of crystals with the typical morphology of in vitro grown HA on the glass surface. In Figure 5C micrographs of SBCu2/AA after 14 days in SBF are reported, showing that even the surface of SBCu2 was covered with crystals at the end of the acellular bioactivity test, confirming that the bioactivity of SBCu2 was not compromised by immersion in AA. These results are in line with EDS results (three area analyses), showing an increase in the peak intensity of P and Ca and an increasing trend in P and Ca amount by increasing the soaking time in SBF (Figure 6). These trends were similar to the ones recorded for glasses before immersion in AA (S2, SB2, and SBCu2), here not reported but available in our previous paper related to the synthesis and characterization of these novel BGs.[39] However, in the case of SBCu2/AA, a small discrepancy with SBCu2 can be observed, being SBCu2/AA characterized by lower values of P and Ca amount, as shown in Figure 6. This discrepancy could be related to the probable release of ions during immersion in acetic acid. In addition, it could also be linked to the specific used analysis technique, the EDS analysis, which is more a qualitative than a quantitative method of the quantification of incorporated ions.

The Ca/P ratio for all glasses (S2/AA, SB2/AA and SBCu2/AA) immersed in SBF was similar to the stoichiometric ratio of HA.

TABLE 2 Diameters of the fibers.

Fiber diameter (μm)	
PCL/AA/S2 (20%)	1.35 ± 0.8
PCL/AA/SB2 (20%)	1.9 ± 0.9
PCL/AA/SBCu2 (20%)	2.2 ± 1.5

3.4 | Water contact-angle measurements

If bioactive glasses are added in a hydrophobic polymer matrix, an increase in the hydrophilicity and water absorption can occur and, as a consequence of such wettability alteration, it has been shown that surface and bulk properties of composite scaffolds can be modified by the incorporation of bioactive glasses. However, to better understand our results, it should be remembered that wettability properties depend not only on the chemical composition of the samples, but also on their roughness and porosity.

In this work, for each kind of electrospun fiber, contact angle (CA) measurements were performed in triplicate. Thus, the CA was calculated as the average of three measurements and the standard deviations were determined, as shown in Figure 7.

Contact angle values of both neat PCL and composite electrospun materials were comparable (according to the Student's *t*-test, the

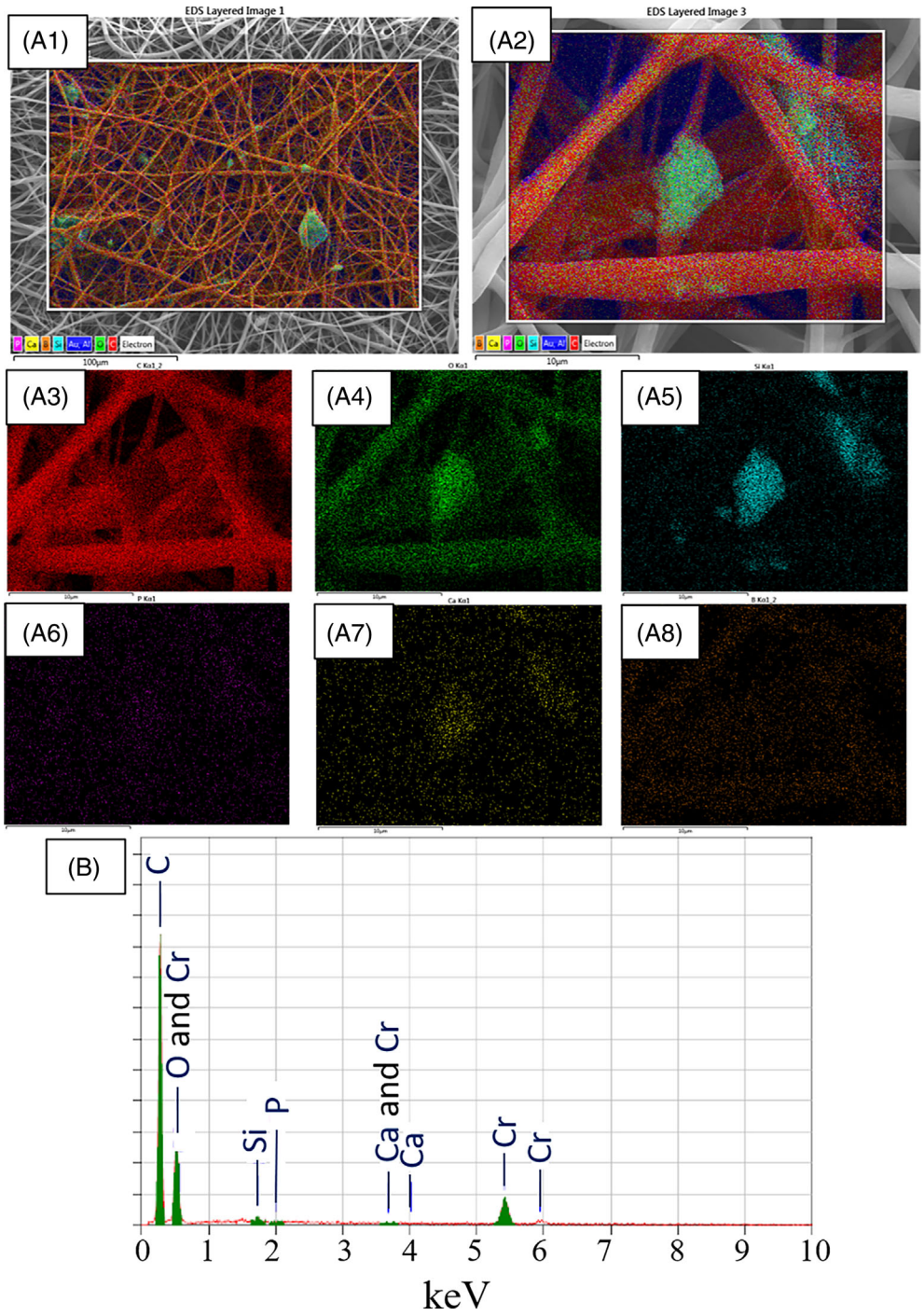

FIGURE 2 EDS mapping (A) and EDS pattern, (B) of PCL/AA/SB2 (20%) fibers where (A.1) all ions distribution at 1 k× of magnification (A.2) all ions distribution at 10 k× magnification (A.3) distribution of carbon, (C) (A.4) distribution of oxygen (O) (A.5) distribution of silicon (Si) (A.6) distribution of phosphorus (P) (A.7) distribution of calcium (Ca) (A.8) distribution of boron (B); in the EDS pattern there are also chromium peaks because the samples were sputtered with chromium to perform the FESEM-EDS analysis.

difference between the measured values were not significative for $p < .05$), showing a hydrophobic behavior, in agreement with literature results.[53] Indeed, the glass nanoparticles were mainly aggregated and not highly homogeneously dispersed in the PCL matrix and the presence of these clusters and the related enhanced roughness of the fiber surface could be the reasons why the composite fibers were still hydrophobic. These results could be positive for the desired antibacterial properties of the composite fibers, because most of the bacterial cells, such as *S. aureus* and *E. coli*, are attracted by hydrophilic surfaces, whereas hydrophobic substrates tend to have an anti-biofouling and antiadhesive behavior against bacteria.

The slight differences in CA values among the composite fibers could be attributed to differences in glass distribution, and to the porosity and deposition of the fibers that were randomly oriented.

3.5 | Mechanical characterization

The mechanical properties of the composite fibers must be studied since they play an essential role for the success of the potential application of the samples, in particular in terms of elastic mismatch between the graft and the host tissue.

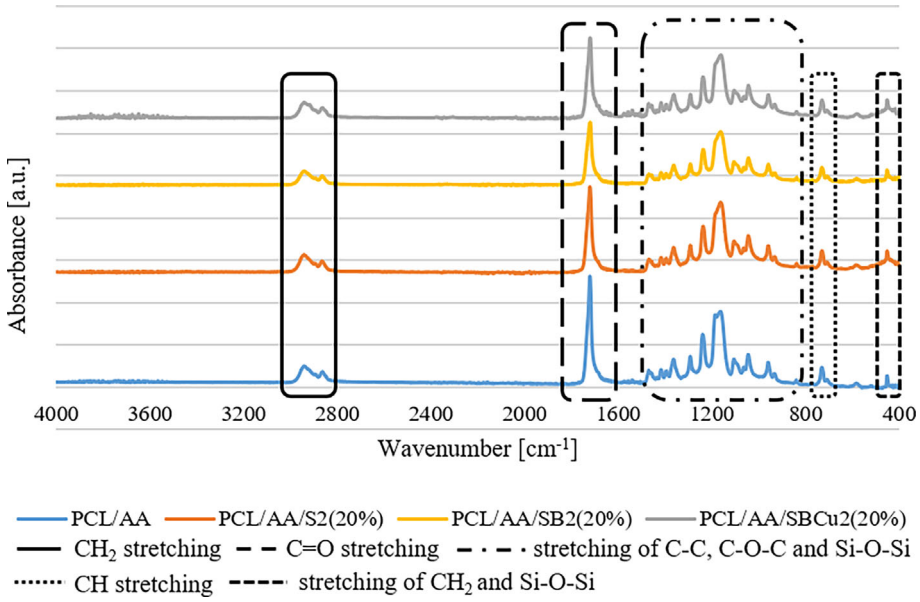

FIGURE 3 FTIR spectra of the electrospun fibers (comparison between neat PCL and composite ones).

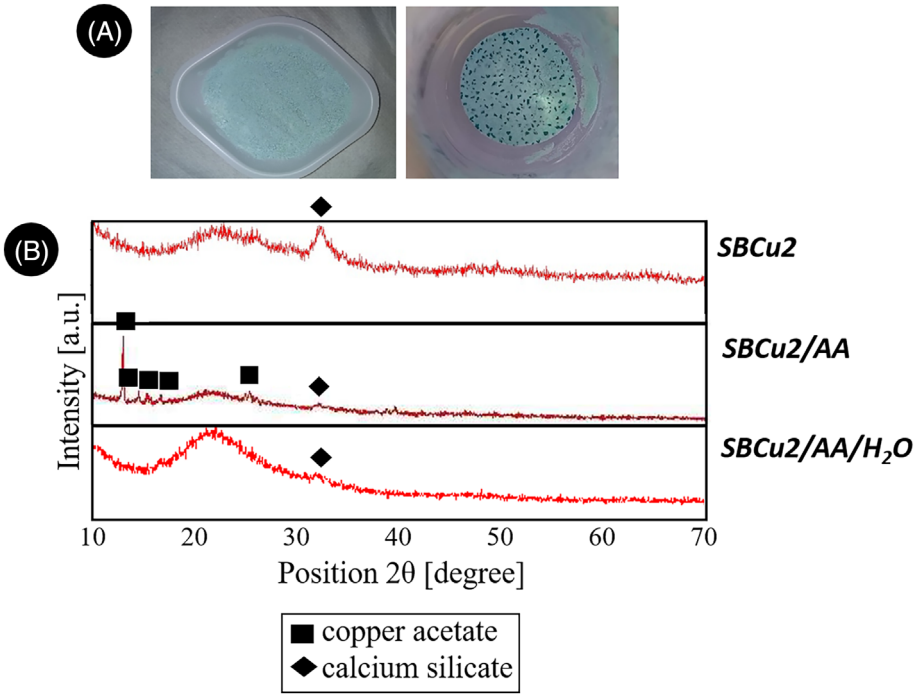

FIGURE 4 (A) SBCu2 before (left) and after (right) immersion in AA and (B) XRD patterns of SBCu2/AA after immersion in AA and SBCu2/AA washed with bi-distilled water where the yellow X shows the peaks of copper acetate.

Mechanical properties values of neat PCL fibers were in agreement with previous experimental results[53,54] and were compared with the ones calculated for the composite fibers, in order to evaluate the effect of the glass addition on the mechanical performance of the materials. In Table 3, results of the mechanical test in terms of force at break, tensile strain at break, ultimate tensile strain (UTS) and elastic modulus (*E*) are reported. Figure 8 shows as example a tensile–stress curve by type of sample, obtained by the uniaxial mechanical tensile test.

In agreement with literature, for both neat polymeric and composite fibers, two linear trends in the stress–strain curve could be observed: a first linear elastic Hookean response caused by the load application and a second non-linear plastic behavior that could be related to the fiber alignment before the sample fracture.[53,55]

As expected from any composite made of a rigid phase in a polymer soft matrix,[26,32,56,57] the measured tensile strain reduction shows that the inclusion of the BG nanoparticles restricted the elongation of the PCL matrix, limiting its plastic deformation, and so provoking a decrease in the elongation at break of the composite fibers.

Regarding the tensile stress, it is possible to observe a significative decrease in the UTS values (Student's *t*-test, $p < .05$) in case of composite fibers.

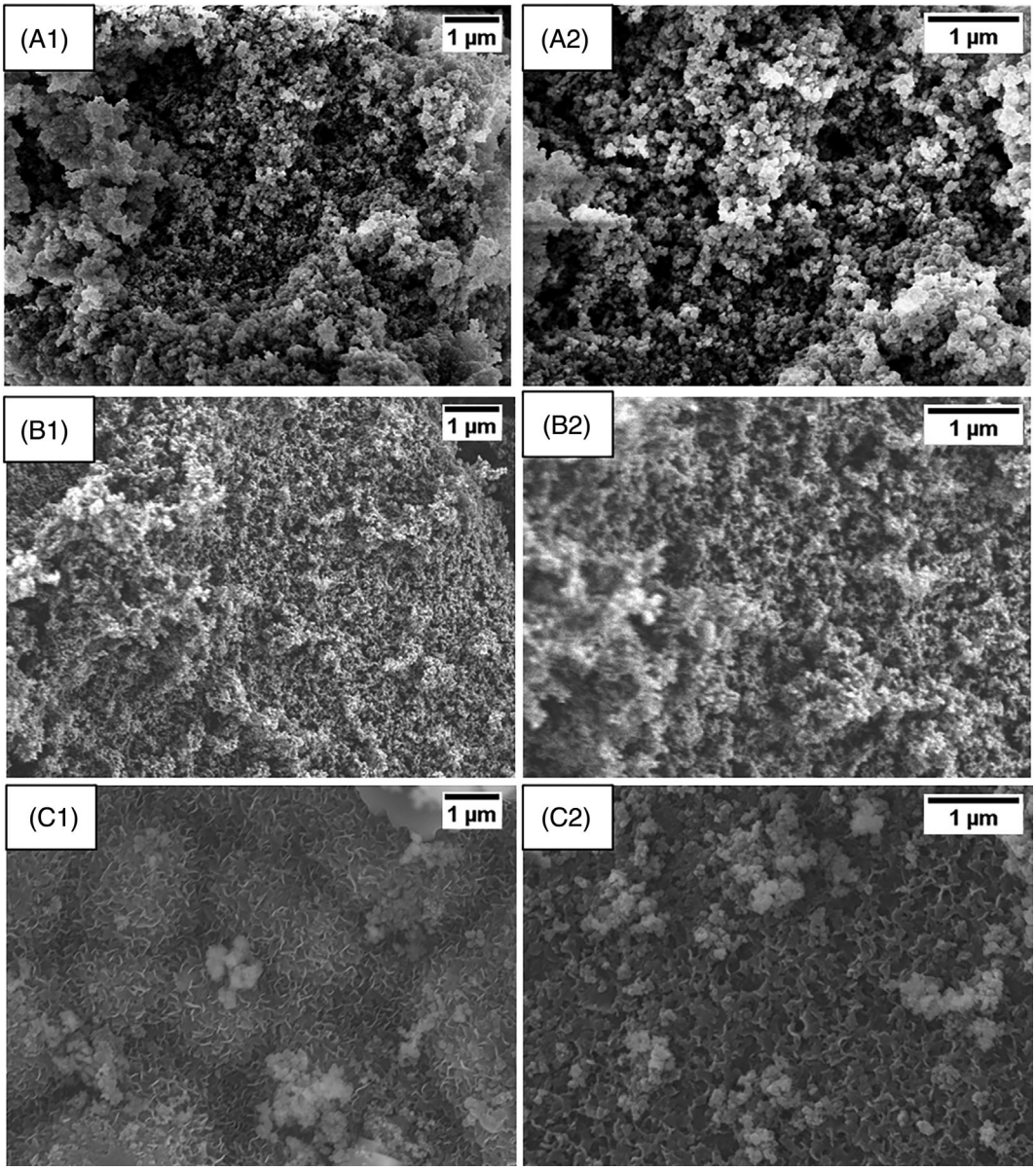

FIGURE 5 FESEM micrographs of (A) SBCu2, (B) SBCu2/AA, and (C) SBCu2/AA after immersion in SBF for up to 14 days: (1) at 30.00 k× and (2) at 50.00 k×.

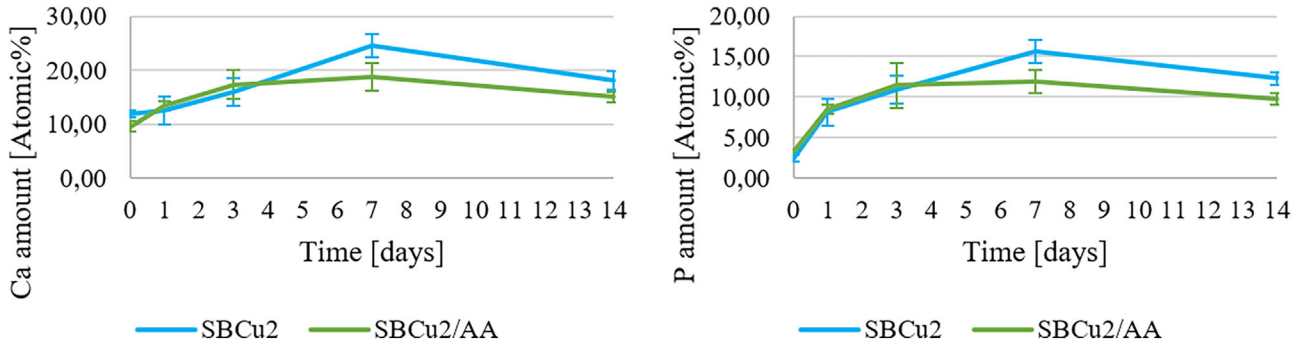

FIGURE 6 EDS results of the stability test: P and Ca amounts versus SBF soaking time—comparison between SBCu2 and SBCu2/AA values ($n = 3$).

Concerning the stiffness of the samples, the elastic modulus *E* of the composite materials was not enhanced, but comparable with literature results.[21,58,59]

The mechanical properties of the composites were satisfying, but sometimes probably influenced by the non-homogeneous distribution of nanoparticles in the PCL matrix due to their partial agglomeration and the poor interaction of the particle clusters with the polymer matrix.[9,60,61] The presence of glass powder clusters can cause local stress concentration regions and the formation of a weak point at the interface between the two materials, lowering the mechanical properties of the composites, as also shown in previous experimental studies.[32,61,62]

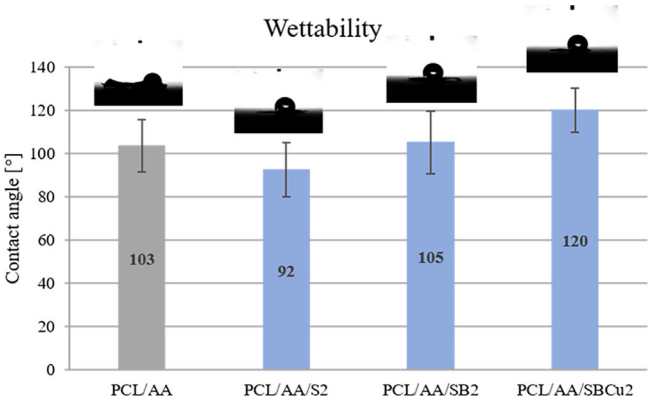

FIGURE 7 Contact angle values for both neat and composite fibers ($n = 3$).

Indeed, the interfacial state between the different phases constituting the composite can significantly affect the mechanical behavior of the composite itself, effectively transferring the load from the matrix to the reinforcement in case of strong interfacial bonding.[63] Moreover, the low *E* values could be caused by a slight increase in the inhomogeneity in the distribution of the average fiber diameter and the presence of roughness on the surface in case of the composite electrospun materials, according to previous results reported by Liverani and Boccaccini.[21]

Finally, the differences between the Young's modulus of the composite scaffolds might originate from different glass dispersion,[28,32,63,64] fiber orientation[27,62,65] and porosity.[65–68] However, these *E* values are very low if compared with the elastic modulus of bone tissue, both cancellous bone ($E = 20$ GPa along the Haversian system and $E = 8$ GPa along the transverse axis) and trabecular porous bone ($E = 0.1$–5 GPa),[18] but adequate to support deformation in scaffolds for soft tissue applications (being in the range 0.4–350 MPa), according to the literature.[24]

The high value of the standard deviation indicates a high distribution of the measured values, suggesting a considerable variability in the mat morphology and glass particle distribution. The variability of the mat could be related to the used electrospinning device, which was very simple to use, but not very sophisticated. In agreement with previous works, this particular device was used, in order to achieve a first evaluation of the interaction between the PCL solution and our novel sol–gel BG nanoparticles and the feasibility of the synthesis of these composite fibers containing such BGs. In any case, the high standard deviation and the low *E* values were not considered so

Sample	Force at break (N)	Tensile strain at break (%)	UTS (MPa)	*E* (MPa)
PCL/AA	0.3 ± 0.1	169 ± 98	3 ± 1	12 ± 2
PCL/AA/S2	0.2 ± 0.0	156 ± 7	1.5 ± 0.3	5 ± 2
PCL/AA/SB2	0.2 ± 0.1	60 ± 41	1.3 ± 0.2	7 ± 2
PCL/AA/SBCu2	0.2 ± 0.0	71 ± 21	1.0 ± 0.1	4 ± 1

TABLE 3 Mechanical properties of both neat and composite fibers ($n = 5$).

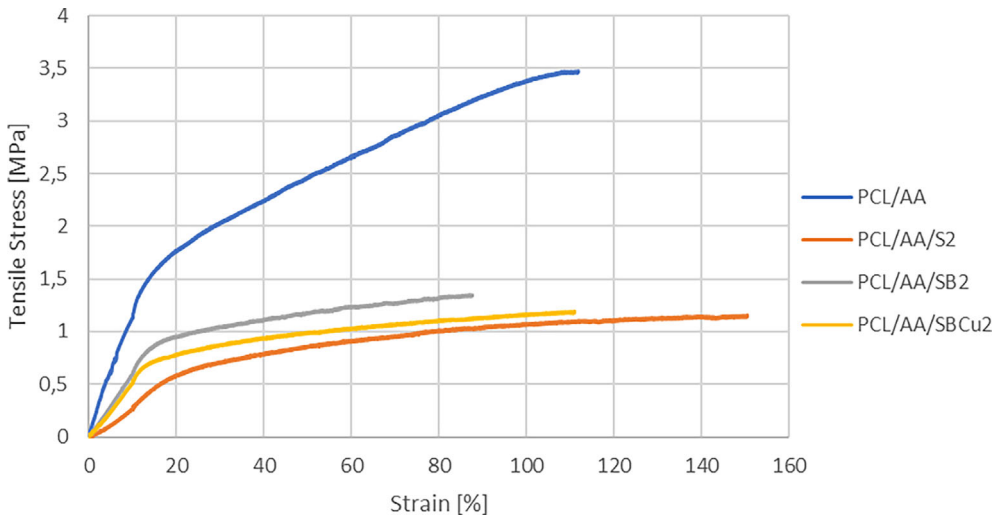

FIGURE 8 Examples of tensile–stress curves obtained by the uniaxial mechanical tensile test.

problematic, since one of the possible applications of these composite fibers could be the regeneration of the interfacial tissues between bone and soft tissues. In addition, from the mechanical point of view, these electrospun materials could be potentially used as wound dressing material. Furthermore, it should be pointed out that observations about the applicability of such composites are in line with what observed from the results of the acellular bioactivity test, explained in the following paragraph.

Regarding the glass distribution inside the PCL matrix, its optimization could be addressed in future works.

3.6 | Acellular bioactivity test

During the acellular bioactivity, the pH trend (here not reported) was almost linear and similar for all investigated samples, with some oscillations of the average measured values in the range between 7.25 and 7.55. From the analysis of the EDS results (reported in Figure 9), an increase in phosphorus and calcium amounts on the sample surface during the soaking time was observed and the morphological analysis confirmed the presence of HA-like crystals on the surface of the composite materials containing S2 (Figure 9A) and SB2 (Figure 9B) at the end of the in vitro bioactivity test (after 21 days of immersion in SBF), whereas it was not possible to detach any HA-like crystals on the surface of PCL/AA/SBCu2 (20%) (Figure 9C). This delayed bioactivity could be attributed to different causes: the presence of copper ions in the glass network[69] or/and the effect of the immersion in AA or/and the slight difference in porosity and thickness of the composite materials, as evaluated from SEM micrography.

FTIR analysis performed on samples immersed in SBF for 1, 3 and 7 days did not show any differences among neat and composite materials, in agreement with SEM-EDS observations, whereas from 14 days in SBF, and in particular after 21 days (Figure 10), it is possible to notice an increase in the intensity of peaks related to P-O-P vibrations, which are located between between 600 and 525 cm^{-1}[39]

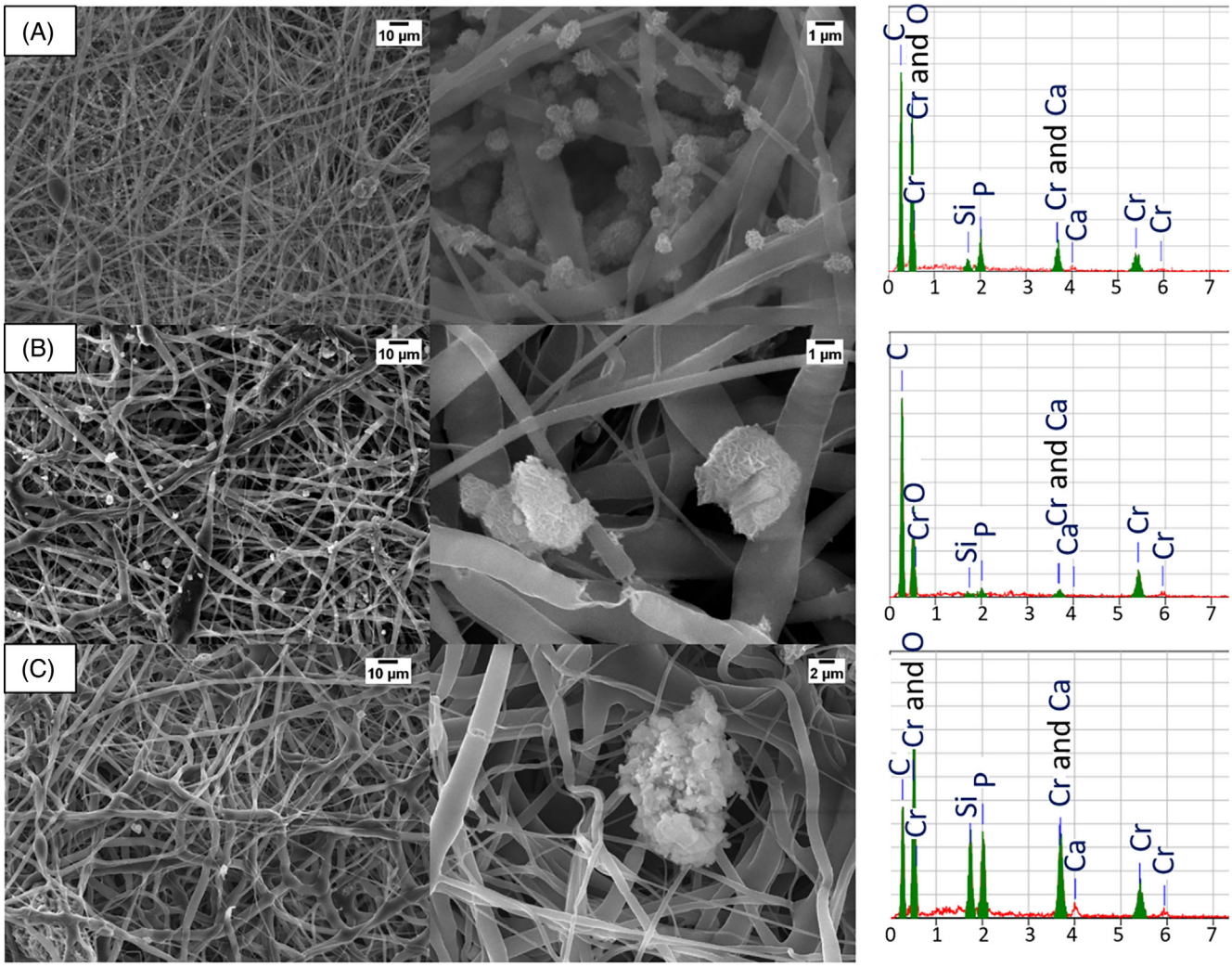

FIGURE 9 SEM micrographs and related EDS pattern of hydroxyapatite crystals on (A) PCL/AA/S2 (20%), (B) PCL/AA/SB2 (20%) and (C) PCL/AA/SBCu2 (20%) after 21 days in SBF.

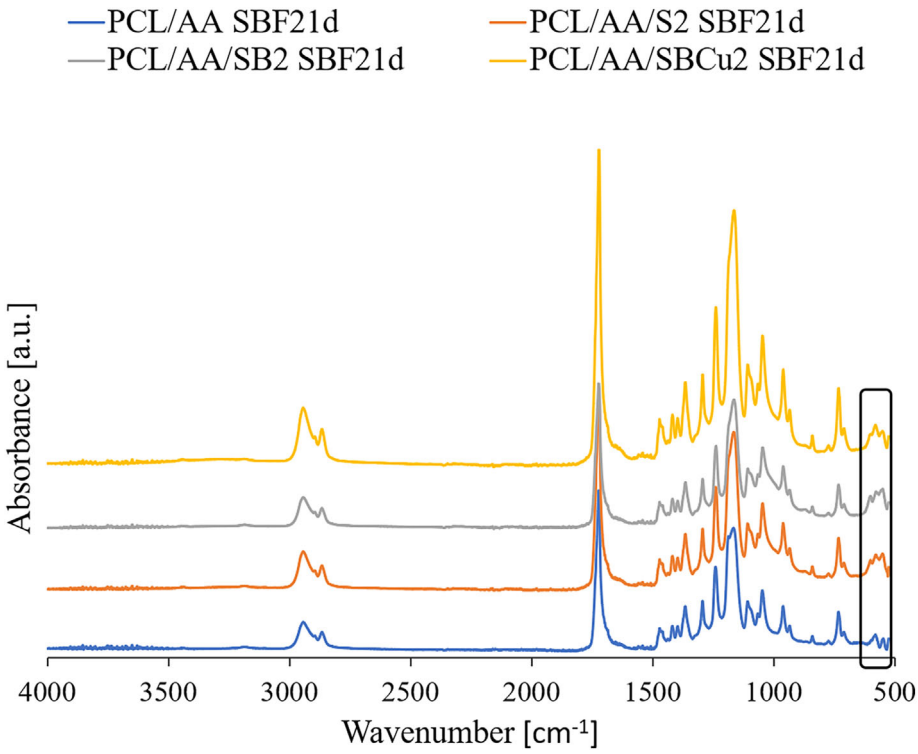

FIGURE 10 FTIR spectra of both neat and composite electrospun fiber mats after 21 days of immersion in SBF (the relevant detected peaks are discussed in the text).

(as highlighted by the circle in Figure 10), indicating the formation of new linkages because of hydroxyapatite deposition on the composite surface.

3.7 | In vitro biodegradation test

The degradation kinetics is affected by various factors, such as chemical composition, molar mass (M_w), polydispersity (M_w/M_n), crystallinity, configurational structure, chain orientation, distribution of chemically reactive compounds within the matrix, presence of additives, processing methods, environmental conditions (such as temperature), buffering capacity, pH, ionic strength, overall hydrophilicity, and device features like size, morphology, and porosity.[8]

The matching between the degradation rate of the scaffold and the regeneration rate of the newly forming tissue is one of the main requirements for a successful tissue regeneration. Thus, degradation and resorption kinetics of each implantable device, including composite scaffolds, must be carefully designed and tailored according to the specific tissue under regeneration. In fact, an ideal scaffold should allow cells to proliferate and secrete their own ECM so that a new functional tissue can form, but this new tissue needs space to grow, thus the scaffold should gradually vanish, leaving free space for new cells responsible for new tissue formation.[9]

PCL is a hydrophobic and highly crystalline polyester, that degrades through random hydrolytic chain scission of the ester linkages in the polymer backbone. Thus, during degradation carboxylic chain ends are created, but only oligomers close to the surface can diffuse out, whereas those in the middle of the structure cannot escape and, remaining inside the chain, act as a catalyst, accelerating the degradation process, which is thus slower at the surface than in the center. Therefore, not allowing fast water penetration into the bulk, in vivo PCL degradation rate is relatively low.[10] Indeed, from Figure 11, it is possible to observe how the extent of degradation was very low, in agreement with literature experimental studies.[55,70]

The insertion of a bioactive glass phase in hydrophobic polymer matrices (such as the PCL ones) should alter the polymer degradation kinetics, causing an increase in the hydrophilicity and hence in the water absorption of the hydrophobic polymer matrix, and consequently, leading to an increase in the hydrolytic degradation of the composite, as shown by many experimental results.[49,57]

However, in this work, bulk erosion process caused by BG addition was not observed. Already before immersion in PBS, some electrospun fibers showed randomly few cracks due to the evaporation of the solvent from the polymer solution during the electrospinning process. By immersion in PBS, the cracks in some cases became bigger. This increase in the size of the cracks could be related to a sort of mechanical degradation, instead of a chemical degradation. Therefore, it is possible that the remaining BG content was insufficient to induce hydrolytic degradation of PCL.

This observation was confirmed by FTIR analysis, which did not show any significant differences among the different analyzed time points.

In agreement with the results of the acellular bioactivity test, no huge variations of solution pH during immersion time were recorded, showing for all the samples an almost linear trend, quite similar to the trend of the control (PBS without any sample) taken as reference.

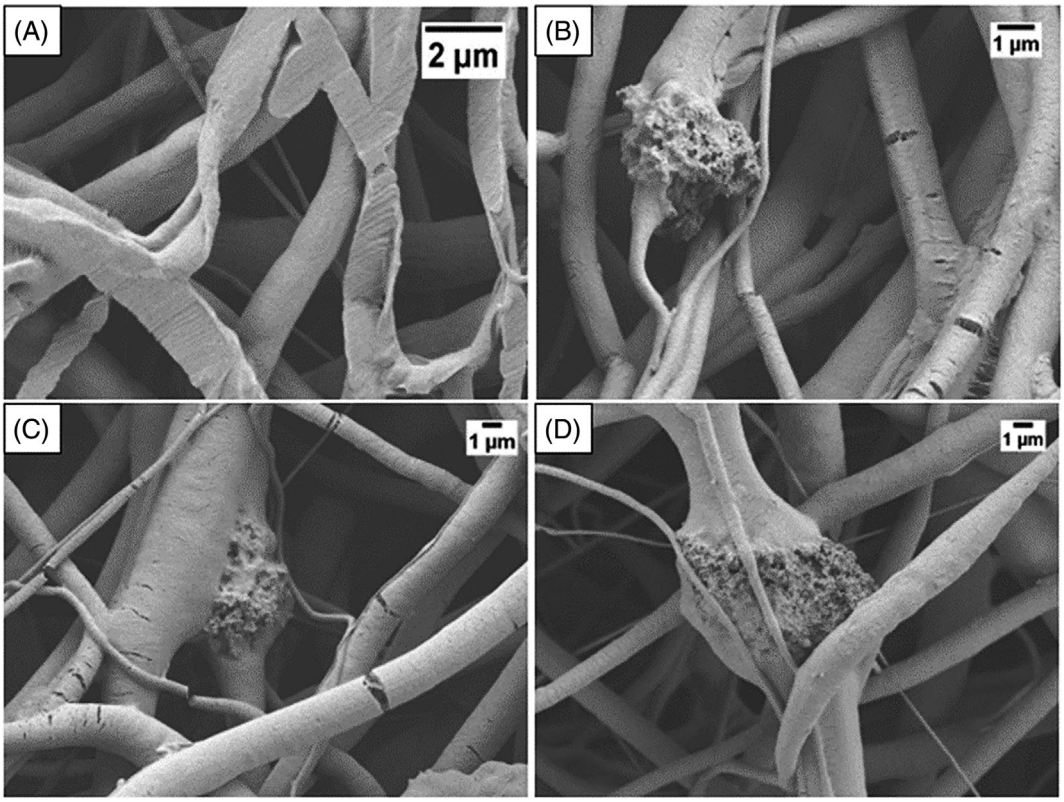

FIGURE 11 SEM micrographs of composite electrospun fibers immersed in PBS for 7 days: (A) PCL/AA PBS 7d, (B) PCL/AA/S2 (20%) PBS 7d, (C) PCL/AA/SB2 (20%) PBS 7d, and (D) PCL/AA/SBCu2 (20%) PBS 7d.

Slight differences in fiber degradation could be attributed to variations in porosity or glass distribution between the composite fibers.

3.8 | Cytocompatibility test

The stromal cell line ST-2, derived from mouse bone marrow, was selected because it has been shown to differentiate in osteoblast,[71,72] chondrocyte,[73] and adipocyte[74,75] phenotypes and it is hence considered a suitable cell line for preliminary assessment (i.e., assessment of cell viability and proliferation) for both soft and hard TE applications.

The preliminary results of the WST-8 assay are reported in Figure 12. After 1 day from the cell seeding (time point 1), cell adhesion and viability of the composite fibers were comparable with the control sample of neat PCL electrospun fibers, not showing any significant difference in the OD values (at 450 nm), with the exception for the composite sample containing SBCu2 glass particles. After 7 days from the seeding, even though the average value of absorbance for the control sample was significantly higher with respect to all the composites, all the composite fibers showed comparable values. Moreover, it is possible to observe a statistically significant increase in the absorbance of all the composite samples respect to the previous time point, in particular in the case of PCL/AA/SB2 (20%), confirming the ability of the cells to proliferate on both neat and composite fibers. Even if the trend of the increase is common to all the samples, the difference between the neat polymeric fibers and the composite one, could be ascribable to a local change of pH due to the presence of BG particles and the related ion release.

The dissolution of bioactive glasses in different solutions due to the ion release has been widely investigated and characterized with particular focus on the effects related to the ion doping, depending on the BGs composition.[76] The ion release influences the pH of the solutions in which the BGs particles or scaffolds are immersed, and in some cases, this change could limit the cell viability. Therefore, a common approach to mitigate this effect is based on the preconditioning of the BG scaffolds before the contact with cell culture.[77]

As reported in the SEM and EDS analyses, BGs and their agglomerates are embedded in the polymeric fibers, affecting the fibers surface topography. Even if it was not measured in this work, the authors supposed an influence of material topography and roughness on cell behavior, as reported in different papers.[78,79]

Fluorescence microscopy confirmed the previous WST-8 test results. Indeed, 7 days after seeding, the morphology of cytoskeletons (stained in red in Figure 12) and nuclei (stained in blue) of seeded proliferating cells were clearly seen thanks to the fluorescence staining. As shown in fluorescence images (reported in Figure 12), vital cells were still present on both pure PCL and composite fibers after 7 days from seeding, confirming the composites were non-toxic. Thus, boron seems to positively affect viability and proliferation of bone murine

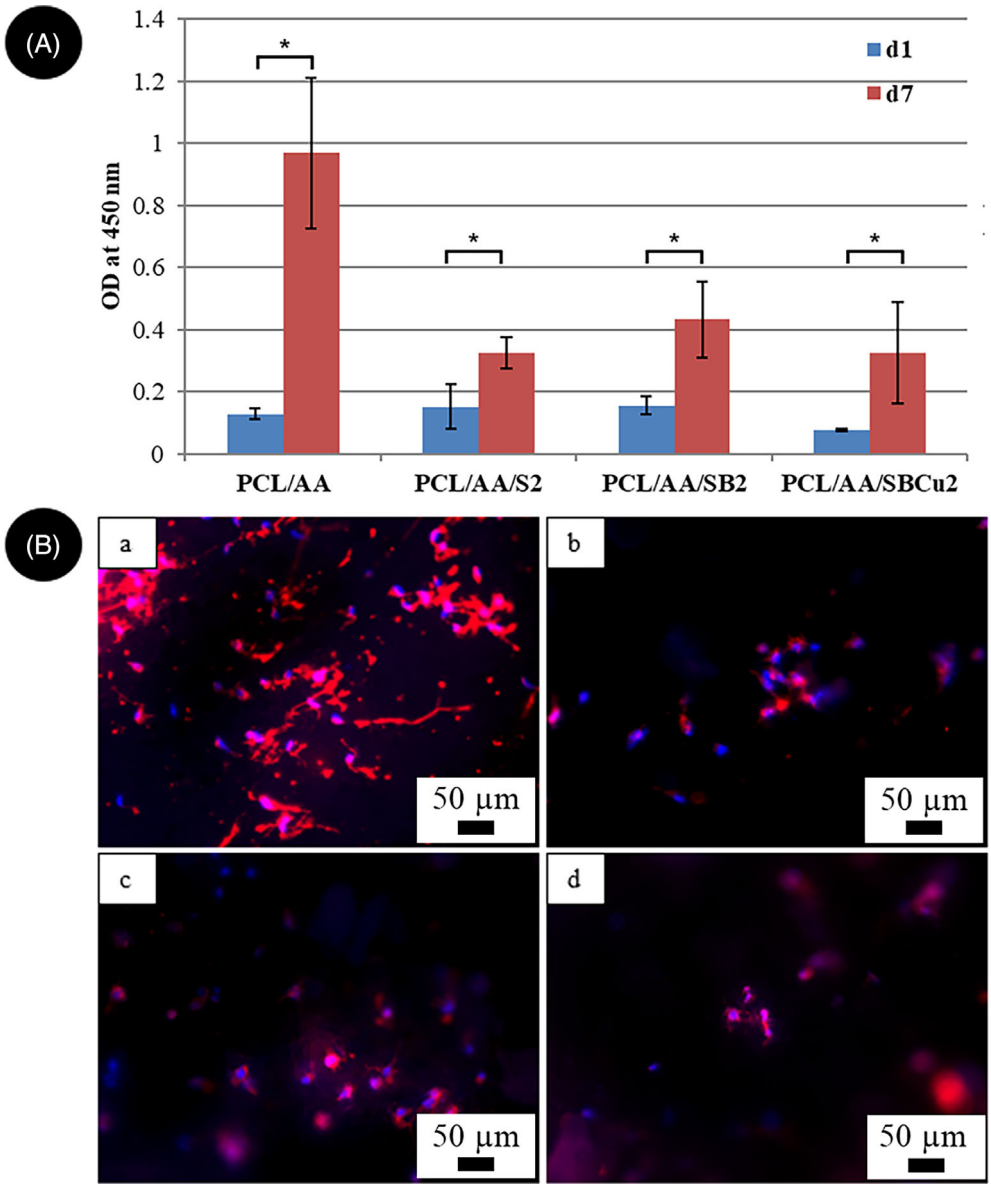

FIGURE 12 (A) WST-8 assay to investigate the viability and the proliferation of the ST-2 cells seeded onto the electrospun materials ($n = 5$), (B) fluorescence microscopy images: (a) PCL/AA, (b) PCL/AA/S2 (20%), (c) PCL/AA/SB2 (20%), and (d) PCL/AA/SBCu2 (20%).

stromal cells, on the contrary of copper, which can be harmful to cells at high concentrations.[80,81]

However, it is important to point out that the proliferation of bone murine stromal cells was allowed on all synthesized composite materials, confirming that they are promising for potential TE applications.

4 | CONCLUSIONS

In this study, three different types of composite electrospun fibers were synthetized and characterized, with the aim of studying the effect of the incorporation of different BGs, doped with boron and with both boron and copper, and fabricating multifunctional fibers.

Among the class of biocompatible and biodegradable synthetic polymers, PCL was selected thanks to its FDA approval for clinical application, ease of fabrication, proper toughness, good flexibility, rheological and viscoelastic properties, and biocompatibility. In order to avoid the use of highly toxic solvents, in this work, the concepts of "green electrospinning" and benign solvents for the electrospinning were adopted and the AA was used as solvent for the polymeric electrospinning solution. A certain degree of particle aggregation was observed. However, despite some clusters of glass particles, the synthesized composite fibrous materials were sufficiently rich in glass powders, that impart bioactivity to the polymeric matrix, allowing the deposition of HA-like crystals on the composite surface. All other tested properties (degradation, mechanical properties, and cytocompatibility) were considered satisfactory.

Issues related to the aggregation of the glass particles have to be investigated and addressed in future works to effectively improve the material properties.

Therefore, from this preliminary study, the newly developed bioactive fibrous composites containing B- and Cu-doped BGs are believed to be potentially useful in TE, due to their bioactivity, soft mechanical properties and the ability to release boron and copper ions from incorporated BG particles, that should impart angiogenic and antibacterial properties to the composites. The obtained fiber mats could be further optimized to enhance glass dispersion and glass incorporation inside the PCL, and the angiogenic and antibacterial properties will be evaluated in future works.

DATA AVAILABILITY STATEMENT

The data that support the findings of this study are available from the corresponding author upon reasonable request.

ORCID

Marta Miola https://orcid.org/0000-0002-1440-6146

REFERENCES

1. Gerhardt LC, Boccaccini AR. Bioactive glass and glass-ceramic scaffolds for bone tissue engineering. *Materials*. 2010;3:3867-3910.
2. Pei B, Wang W, Fan Y, Wang X, Watari F, Li X. Fiber-reinforced scaffolds in soft tissue engineering. *Regen Biomater*. 2017;4:257-268.
3. Vacanti JP, Langer R. Tissue engineering: the design and fabrication of living replacement devices for surgical reconstruction and transplantation. *Lancet*. 1999;354:32-34.
4. Chen Q, Roether JA, Boccaccini ARR. Tissue engineering scaffolds from bioactive glass and composite materials. *Top Tissue Eng*. 2008;4:1-27.
5. Gentile P, Mattioli-Belmonte M, Chiono V, et al. Bioactive glass/polymer composite scaffolds mimicking bone tissue. *J Biomed Mater Res – Part A*. 2012;100:2654-2667.
6. Guarino V, Causa F, Ambrosio L. Bioactive scaffolds for bone and ligament tissue. *Expert Rev Med Devices*. 2007;4:405-418.
7. Chan BP, Leong KW. Scaffolding in tissue engineering: general approaches and tissue-specific considerations. *Eur Spine J*. 2008;17:467-479.
8. Rezwan K, Chen QZ, Blaker JJ, Boccaccini AR. Biodegradable and bioactive porous polymer/inorganic composite scaffolds for bone tissue engineering. *Biomaterials*. 2006;27:3413-3431.
9. Zhou H, Lawrence JG, Bhaduri SB. Fabrication aspects of PLA-CaP/PLGA-CaP composites for orthopedic applications: a review. *Acta Biomater*. 2012;8:1999-2016.
10. Tan L, Yu X, Wan P, Yang K. Biodegradable materials for bone repairs: a review. *J Mater Sci Technol*. 2013;29:503-513.
11. Ramakrishna S, Mayer J, Wintermantel E, Leong KW. Biomedical applications of polymer-composite materials: a review. *Compos Sci Technol*. 2001;61:1189-1224.
12. Kim HW, Lee EJ, Jun IK, Kim HE, Knowles JC. Degradation and drug release of phosphate glass/polycaprolactone biological composites for hard-tissue regeneration. *J Biomed Mater Res – Part B Appl Biomater*. 2005;75:34-41.
13. Kargozar S, Mozafari M, Hill RG, et al. Synergistic combination of bioactive glasses and polymers for enhanced bone tissue regeneration. *Mater Today Proc*. 2018;5:15532-15539.
14. Wang M. Developing bioactive composite materials for tissue replacement. *Biomaterials*. 2003;24:2133-2151.
15. Deliormanlı AM, Yıldırım M. Sol-gel synthesis of 13-93 bioactive glass powders containing therapeutic agents. *J Aust Ceram Soc*. 2016;52:9-19.
16. Shah FA, Czechowska J. Bioactive glass and glass-ceramic scaffolds for bone tissue engineering. *Bioactive Glasses Materials, Properties and Applications*. 2nd ed. Elsevier Ltd; 2018:201-233.
17. Fiume E, Barberi J, Verné E, Baino F. Bioactive glasses: from parent 45S5 composition to scaffold-assisted tissue-healing therapies. *J Funct Biomater*. 2018;9:2-33.
18. Rahaman MN, Day DE, Bal BS, et al. Bioactive glass in tissue engineering. *Acta Biomater*. 2011;7:2355-2373.
19. Kim HW, Kim HE, Knowles JC. Production and potential of bioactive glass nanofibers as a next-generation biomaterial. *Adv Funct Mater*. 2006;16:1529-1535.
20. Balakrishnan P, Gardella L, Forouharshad M, Pellegrino T, Monticelli O. Star poly(ε-caprolactone)-based electrospun fibers as biocompatible scaffold for doxorubicin with prolonged drug release activity. *Colloids Surf B: Biointerfaces*. 2018;161:488-496.
21. Liverani L, Boccaccini AR. Versatile production of poly(epsilon-caprolactone) fibers by electrospinning using benign solvents. *Nanomaterials*. 2016;6:1-15.
22. Jiang T, Carbone EJ, Lo KWH, Laurencin CT. Electrospinning of polymer nanofibers for tissue regeneration. *Prog Polym Sci*. 2015;46:1-24.
23. Haider A, Haider S, Kang IK. A comprehensive review summarizing the effect of electrospinning parameters and potential applications of nanofibers in biomedical and biotechnology. *Arab J Chem*. 2018;11:1165-1188.
24. Kenry LCT. Nanofiber technology: current status and emerging developments. *Prog Polym Sci*. 2017;70:1-17.
25. Liverani L, Killian MS, Boccaccini AR. Fibronectin functionalized electrospun fibers by using benign solvents: best way to achieve effective functionalization. *Front Bioeng Biotechnol*. 2019;7:1-12.
26. Kang MS, Kim J-HH, Singh RK, et al. Therapeutic-designed electrospun bone scaffolds: mesoporous bioactive nanocarriers in hollow fiber composites to sequentially deliver dual growth factors. *Acta Biomater*. 2015;16:103-116.
27. Liverani L, Lacina J, Roether JA, et al. Incorporation of bioactive glass nanoparticles in electrospun PCL/chitosan fibers by using benign solvents. *Bioact Mater*. 2018;3:55-63.
28. Serio F, Miola M, Verné E, Pisignano D, Boccaccini AR, Liverani L. Electrospun filaments embedding bioactive glass particles with ion release and enhanced mineralization. *Nanomaterials*. 2019;9:1-15.
29. Gerhardt LC, Widdows KL, Erol MM, et al. The pro-angiogenic properties of multi-functional bioactive glass composite scaffolds. *Biomaterials*. 2011;32:4096-4108.
30. Kargozar S, Baino F, Hamzehlou S, Hill RG, Mozafari M. Bioactive glasses: prouting angiogenesis in tissue engineering. *Trends Biotechnol*. 2018;36:430-444.
31. Deliormanlı AM. Electrospun cerium and gallium-containing silicate based 13-93 bioactive glass fibers for biomedical applications. *Ceram Int*. 2016;42:897-906.
32. Moura D, Souza MT, Liverani L, et al. Development of a bioactive glass-polymer composite for wound healing applications. *Mater Sci Eng C*. 2017;76:224-232.
33. Ciraldo FE, Liverani L, Gritsch L, Goldmann WH, Boccaccini AR. Synthesis and characterization of silver-doped mesoporous bioactive glass and its applications in conjunction with electrospinning. *Materials*. 2018;11:1-16.
34. Zhou J, Wang H, Zhao S, et al. In vivo and in vitro studies of borate based glass micro-fibers for dermal repairing. *Mater Sci Eng C*. 2016;60:437-445.
35. Balasubramanian P, Büttner T, Miguez Pacheco V, Boccaccini AR. Boron-containing bioactive glasses in bone and soft tissue engineering. *J Eur Ceram Soc*. 2018;38:855-869.
36. Luo Y, Wu C, Lode A, Gelinsky M. Hierarchical mesoporous bioactive glass/alginate composite scaffolds fabricated by three-dimensional plotting for bone tissue engineering. *Biofabrication*. 2013;5:1-14.

37. Bari A, Bloise N, Fiorilli S, et al. Copper-containing mesoporous bioactive glass nanoparticles as multifunctional agent for bone regeneration. *Acta Biomater*. 2017;55:493-504.
38. Miola M, Bertone E, Verné E. In situ chemical and physical reduction of copper on bioactive glass surface. *Appl Surf Sci*. 2019;495:2-14.
39. Piatti E, Verné E, Miola M. Synthesis and characterization of sol-gel bioactive glass nanoparticles doped with boron and copper. *Ceram Int*. 2022;48:13706-13718.
40. Access O, Lepry WC, Smith S, Liverani L, Boccaccini AR, Nazhat SN. Acellular bioactivity of sol-gel derived borate glass-polycaprolactone electrospun scaffolds. *Biomed Glas*. 2016;2:88-98.
41. Akturk A, Erol Taygun M, Goller G. Optimization of the electrospinning process variables for gelatin/silver nanoparticles/bioactive glass nanocomposites for bone tissue engineering. *Polym Compos*. 2020;41:2411-2425.
42. Schneider CA, Rasband WS, Eliceiri KW. NIH image to ImageJ: 25 years of image analysis. *Nat Methods*. 2012;7:671-675.
43. Kokubo T, Takadama H. How useful is SBF in predicting in vivo bone bioactivity? *Biomaterials*. 2006;27:2907-2915.
44. Zhou X, Li J, Sun H, Hu Y, Che L, Wang Z. Controlled cell patterning on bioactive surfaces with special wettability. *J Bionic Eng*. 2017;14:440-447.
45. Bacakova L, Filova E, Parizek M, Ruml T, Svorcik V. Modulation of cell adhesion, proliferation and differentiation on materials designed for body implants. *Biotechnol Adv*. 2011;29:739-767.
46. Yang N, Yang MK, Bi SX, et al. Cells behaviors and genotoxicity on topological surface. *Mater Sci Eng C*. 2013;33:3465-3473.
47. Premnath P, Tavangar A, Tan B, Venkatakrishnan K. Tuning cell adhesion by direct nanostructuring silicon into cell repulsive/adhesive patterns. *Exp Cell Res*. 2015;337:44-52.
48. Jaggessar A, Shahali H, Mathew A, Yarlagadda PKDV. Bio-mimicking nano and micro-structured surface fabrication for antibacterial properties in medical implants. *J Nanobiotechnol*. 2017;15:1-20.
49. Yang Y, Michalczyk C, Singer F, Virtanen S, Boccaccini AR. In vitro study of polycaprolactone/bioactive glass composite coatings on corrosion and bioactivity of pure Mg. *Appl Surf Sci*. 2015;355:832-841.
50. Luginina M, Schuhladen K, Orrú R, Cao G, Boccaccini AR, Liverani L. Electrospun PCL/PGS composite fibers incorporating bioactive glass particles for soft tissue engineering applications. *Nanomaterials*. 2020;10:1-18.
51. Li W, Shi L, Zhang X, Liu K, Ullah I, Cheng P. Electrospinning of polycaprolactone nanofibers using H_2O as benign additive in polycaprolactone/glacial acetic acid solution. *J Appl Polym Sci*. 2018;135:1-9.
52. Li M, Mondrinos MJ, Chen X, Gandhi MR, Ko FK, Lelkes PI. Co-electrospun poly(lactide-co-glycolide), gelatin, and elastin blends for tissue engineering scaffolds. *J Biomed Mater Res Part A*. 2006;7(9):963-973.
53. Liverani L, Boccardi E, Beltrán AM, Boccaccini AR. Incorporation of calcium containing mesoporous (MCM-41-type) particles in electrospun PCL fibers by using benign solvents. *Polymers*. 2017;9:1-16.
54. Ekaputra AK, Zhou Y, Cool SMK, Hutmacher DW. Composite electrospun scaffolds for engineering tubular bone grafts. *Tissue Eng – Part A*. 2009;15:3779-3788.
55. Dulnik J, Denis P, Sajkiewicz P, Kołbuk D, Choinska B. Biodegradation of bicomponent PCL/gelatin and PCL/collagen nano fibers electrospun from alternative solvent system. *Polym Degrad Stab*. 2016;130:10-21.
56. Otadi M, Mohebbi-Kalhori D. Evaluate of different bioactive glass on mechanical properties of nanocomposites prepared using electrospinning method. *Procedia Mater Sci*. 2015;11:196-201.
57. Kouhi M, Morshed M, Varshosaz J, Fathi MH. Poly (ε-caprolactone) incorporated bioactive glass nanoparticles and simvastatin nanocomposite nanofibers: preparation, characterization and in vitro drug release for bone regeneration applications. *Chem Eng J*. 2013;228:1057-1065.
58. Sergi R, Cannillo V, Boccaccini AR, Liverani L. Incorporation of bioactive glasses containing Mg, Sr, and Zn in electrospun PCL fibers by using benign solvents. *Appl Sci*. 2020;10:1-19.
59. Chen S, Galusková D, Kaňková H, et al. Electrospun PCL fiber mats incorporating multi-targeted B and Co co-doped bioactive glass nanoparticles for angiogenesis. *Materials*. 2020;13:1-15.
60. Conoscenti G, Carfì Pavia F, Ciraldo FE, et al. In vitro degradation and bioactivity of composite poly-L-lactic (PLLA)/bioactive glass (BG) scaffolds: comparison of 45S5 and 1393BG compositions. *J Mater Sci*. 2018;53:2362-2374.
61. Jo JH, Lee EJ, Shin DS, et al. In vitro/in vivo biocompatibility and mechanical properties of bioactive glass nanofiber and poly(ε-caprolactone) composite materials. *J Biomed Mater Res – Part B Appl Biomater*. 2009;91:213-220.
62. Tansaz S, Liverani L, Vester L, Boccaccini AR. Soy protein meets bioactive glass: electrospun composite fibers for tissue engineering applications. *Mater Lett*. 2017;199:143-146.
63. Šupová M. Problem of hydroxyapatite dispersion in polymer matrices: a review. *J Mater Sci Mater Med*. 2009;20:1201-1213.
64. Nejati E, Firouzdor V, Eslaminejad MB, Bagheri F. Needle-like nano hydroxyapatite/poly(L-lactide acid) composite scaffold for bone tissue engineering application. *Mater Sci Eng C*. 2009;29:942-949.
65. Croisier F, Duwez A, Jérôme C, et al. Mechanical testing of electrospun PCL fibers. *Acta Biomater*. 2012;8:218-224.
66. Karageorgiou V, Kaplan D. Porosity of 3D biomaterial scaffolds and osteogenesis. *Biomaterials*. 2005;26:5474-5491.
67. Wutticharoenmongkol P, Sanchavanakit N, Pavasant P, Supaphol P. Preparation and characterization of novel bone scaffolds based on electrospun polycaprolactone fibers filled with nanoparticles. *Macromol Biosci*. 2006;6:70-77.
68. Zhang K, Wang Y, Hillmyer MA, Francis LF. Processing and properties of porous poly(L-lactide)/bioactive glass composites. *Biomaterials*. 2004;25:2489-2500.
69. Bejarano J, Caviedes P, Palza H. Sol-gel synthesis and in vitro bioactivity of copper and zinc-doped silicate bioactive glasses and glass-ceramics. *Biomed Mater*. 2015;10:1-13.
70. Shirani K, Nourbakhsh MSS, Rafienia M. Electrospun polycaprolactone/gelatin/bioactive glass nanoscaffold for bone tissue engineering. *Int J Polym Mater Polym Biomater*. 2018;4037:1-9.
71. Otsuka E, Yamaguchi A, Hirose S, Hagiwara H. Characterization of osteoblastic differentiation of stromal cell line ST2 that is induced by ascorbic acid. *Am J Physiol – Cell Physiol*. 1999;277:132-138.
72. Koike M, Shimokawa H, Kanno Z, Ohya K, Soma K. Effects of mechanical strain on proliferation and differentiation of bone marrow stromal cell line ST2. *J Bone Miner Metab*. 2005;23:219-225.
73. Robins JC, Akeno N, Mukherjee A, et al. Hypoxia induces chondrocyte-specific gene expression in mesenchymal cells in association with transcriptional activation of Sox9. *Bone*. 2005;37:313-322.
74. Ding J, Nagai K, Woo J-T. Insulin-dependent adipogenesis in stromal ST2 cells derived from murine bone marrow. *Biosci Biotechnol Biochem*. 2003;67:314-321.
75. Huang J, Zhao L, Xing L, Chen D. MicroRNA-204 regulates Runx2 protein expression and mesenchymal progenitor cell differentiation. *Stem Cells*. 2010;28:357-364.
76. Schuhladen K, Wang X, Hupa L, Boccaccini AR. Dissolution of borate and borosilicate bioactive glasses and the influence of ion (Zn, Cu) doping in different solutions. *J Non Cryst Solids*. 2018;502:22-34.
77. Ciraldo FE, Boccardi E, Melli V, Westhauser F, Boccaccini AR. Tackling bioactive glass excessive in vitro bioreactivity: preconditioning approaches for cell culture tests. *Acta Biomater*. 2018;75:3-10. doi: 10.1016/j.actbio.2018.05.019

78. Cai S, Wu C, Yang W, Liang W, Yu H, Liu L. Recent advance in surface modification for regulating cell adhesion and behaviors. *Nanotechnol Rev*. 2020;9:971-989.
79. Majhy B, Priyadarshini P, Sen AK. Effect of surface energy and roughness on cell adhesion and growth – facile surface modification for enhanced cell culture. *R Soc Chem Adv*. 2021;11:15467-15476.
80. Wu C, Zhou Y, Xu M, et al. Copper-containing mesoporous bioactive glass scaffolds with multifunctional properties of angiogenesis capacity, osteostimulation and antibacterial activity. *Biomaterials*. 2013;34:422-433.
81. Ali A, Ershad M, Vyas VK, et al. Studies on effect of CuO addition on mechanical properties and in vitro cytocompatibility in 1393 bioactive glass scaffold. *Mater Sci Eng C*. 2018;93:341-355.

How to cite this article: Piatti E, Miola M, Liverani L, Verné E, Boccaccini AR. Poly(ε-caprolactone)/bioactive glass composite electrospun fibers for tissue engineering applications. *J Biomed Mater Res*. 2023;111(11):1692-1709. doi:10.1002/jbm.a.37578